TAO, Vol.7, No.1, 13-29, March 1996

The 16 September 1994 Earthquake (m_b=6.5) in the Taiwan Strait and Its Tectonic Implications

HONN KAO[1] and FRANCIS T. WU[2]

(Manuscript received 13 June 1995, in final form 30 September 1995)

ABSTRACT

The 16 September 1994 earthquake, with its epicenter located ~150 km southwest of Taiwan in the western part of the Tainan Basin, has been the largest event (m_b=6.5) in the Taiwan Strait in modern history. There were several known large historical earthquakes in the Taiwan Strait, but in the epicentral area there was no known historical seismicity and the present day seismicity is not noticeably higher than in other area of the Strait. The focal mechanism of this event (strike, 103±17; dip, 55±5; rake, -74±16) is obtained by inverting both teleseismic P and SH waveforms. The solution is a high-angle, normal fault with the two nodal planes striking approximately east-west, implying north-south extension in the source region. The estimated centroid depth is 13±3 km, consistent with that reported in the Preliminary Determination of Epicenter (PDE). The source time function is a very simple triangle of only 2.4 s in duration, and the seismic moment is $7.0\pm1.1 \times 10^{18}$ Nt m. Based on the aftershock distribution, we infer that the earthquake probably took place along the south-dipping nodal plane. However, due to the large uncertainty in the hypocentral locations of aftershocks, the precise geometry of the rupture area is not resolvable. By assuming the densest aftershock zone to be the rupture area (~15 km long by 20 km wide), the inferred stress drop is ~33 bar. On the other hand, the calculated stress drop is as high as 3.8 kbar if it is assumed that the rupture area is the square of the product of the half duration of the source time function and the rupture velocity (Kikuchi and Fukao, 1988). The corner frequency of the displacement spectrum recovered by the broadband seismogram recorded at a close-in station (PNG) is consistent with the higher stress drop. Nonetheless, lower values cannot be completely ruled out. We interpret the earthquake as a consequence of the northsouth extension perpendicular to the σ_1 for the

[1] Institute of Earth Sciences, Academia Sinica P. O. Box 1-55, Nankang, Taipei, Taiwan, R.O.C.

[2] Department of Geological Sciences, State University of New York at Binghamton, Binghamton, New York, U.S.A.

arc-continent collision near Taiwan. An analogous extensional environment is found in the high Tibet plateau north of the Himalayan collision zone. It is concluded that normal faults in the Tainan Basin are active and capable of generating large earthquakes. After the initial rifting stage and later post-rift phase of thermal subsidence, the Tainan Basin is now in a syn-collisional stage not asimilar to that in the Tibet plateau.

(Key words: Earthquake source parameters, Waveform inversion, Collision zone, Taiwan strait)

1. INTRODUCTION

Seismicity in the Taiwan region reflects the complex tectonic interaction between the Eurasia plate and the Philippine Sea plate. In the vicinity of Taiwan, the Philippine Sea plate moves in the N50°W direction at a rate of 7±4 cm yr^{-1} (e.g., Huchon, 1986; Karig and Cardwell, 1986; Minster and Jordan, 1979; Ranken *et al.*, 1984; Seno, 1977; Seno *et al.*, 1987, 1993; Figure 1). While this plate subducts northwesterly beneath the Eurasia plate along much of the Ryukyu trench, after the subduction zone changes its strike from northeast-southwest to nearly east-west as it approaches Taiwan, the continued motion of the Philippine Sea plate leads to the collision of this plate with the Eurasia plate between Hualien and Taitung. The arc-continent collision has been the dominant feature since ~4 Ma (e.g., Bowin *et al.*, 1978; Ho, 1986; Lee and Lawver, 1994; Teng, 1990; Wu, 1978). To the south of Taiwan, the north Luzon arc-Manila trench system is associated with the Eurasia plate subducting eastward beneath the Philippine Sea plate. This subduction system extends northward under the southern tip of Taiwan, south of Taitung. The subduction zone under northern Taiwan and the collision-associated structures are clearly shown in tomographic images (e.g., Rau and Wu, 1995; Roecker *et al.*, 1987).

Although the relation between the overall active tectonics and seismicity in the vicinity of Taiwan is clear, the infrequent yet persistent seismicity in the Taiwan Strait has not been adequately investigated (Wu *et al.*, 1991). The Strait, which is situated on the continental margin of southeast China (Figures 1 and 2), has had several large ($M \geq 6$) earthquakes in historical time, the best known event being the 1604 $M \approx 8$ Quanzhou earthquake (Lee *et al.*, 1976, 1978). Since 1961, when high quality analog World-Wide Standardized Seismograph Network (WWSSN) records became available, no events with $m_b \geq 5.5$ have occurred in the Taiwan Strait. Therefore, while intraplate earthquakes (i.e., events more than 100 km away from the nearest plate boundary) may be very important in understanding the compleat collisional tectonics of Taiwan, the lack of information concerning the sources of the historical events (including the epicentral locations, focal depths, and focal mechanisms) makes it difficult to assess the role these events actually play.

The occurrence of a large intraplate earthquake on 16 September 1994 approximately 150 km southwest of Taiwan (Figures 1 and 2) changed this situation. This event is deemed a rarity not only for its unusual hypocentral location, but also for its large magnitude (m_b=6.5). The epicenter reported by the Central Weather Bureau (CWB) of Taiwan, using local data, is at 22.43°N, 118.47°E, which is approximately 27 km southwest of the one (22.53°N, 118.71°E) listed in the Preliminary Determination of Epicenters (PDE) of the U.S. Geological Survey (USGS), based on global data. The epicentral area of this event has never been known for either modern or historical seismicity (Figure 2). Multichannel seismic lines in this area, however, have revealed numerous normal faults in the region (e.g., Yang *et al.*, 1991).

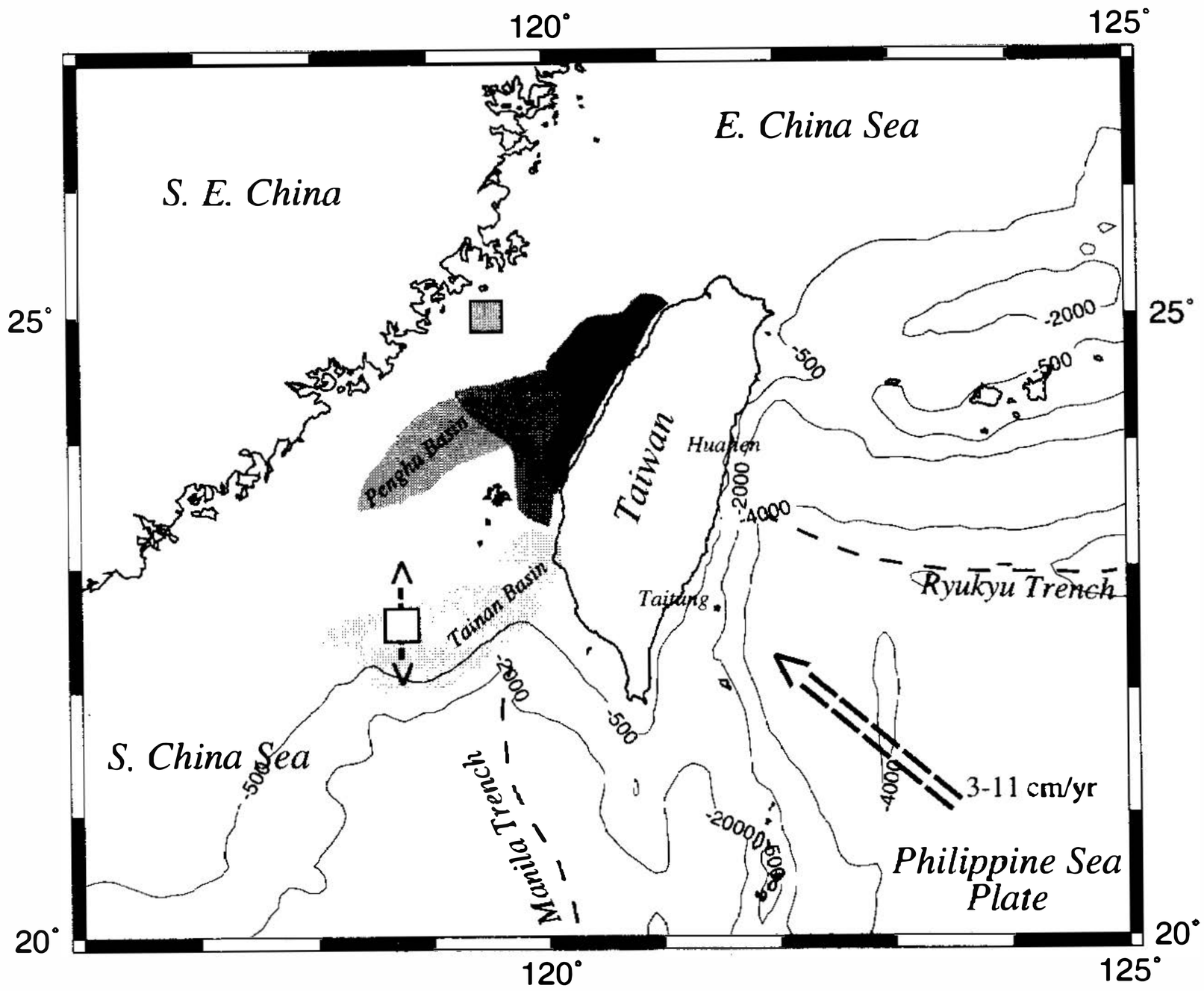

Fig. 1. Map showing the geologic and tectonic settings near Taiwan. The Philippine Sea plate moves toward the northwest at a rate of 7±4 cm yr^{-1} relative to the Eurasia plate (big arrow). The approximate locations of the Ryukyu and Manila trenches are marked by dashed lines. In the Taiwan Strait, major geological structures are marked by gray regions (the Taishi, Penghu, and Tainan Basins; and the Penghu Uplift). The 16 September 1994 earthquake (open square) was located in the western part of the Tainan Basin with the *T*-axis oriented approximately north-south (small arrows). The gray square shows the epicenter of the 1604 Quanzhou earthquake, which has been the largest event in the region.

In this study, the geological and tectonic setting in the epicentral area of the 16 September 1994 event is first introduced briefly . Then we investigate the source characteristics of this earthquake in some detail, including a concise description of our waveform analysis. Finally, the tectonic implications are discussed in terms of the relationship between the strain field in the Taiwan Strait and the dominant arc-continent collision to the east, as well as the active orogeny on the island. Specifically, we shall explore the analogy between this event and normal faults found in high Tibet behind the continent-continent collision zone along the Himalayas.

2. TECTONICS AND HISTORICAL SEISMICITY OF THE TAIWAN STRAIT

The Taiwan Strait is situated on the continental shelf off the southeast China coast between the East China Sea and the South China Sea with an average water depth of less than 200 m (Figure 1). West of Taiwan, there are two major basin systems, the Taihsi Basin

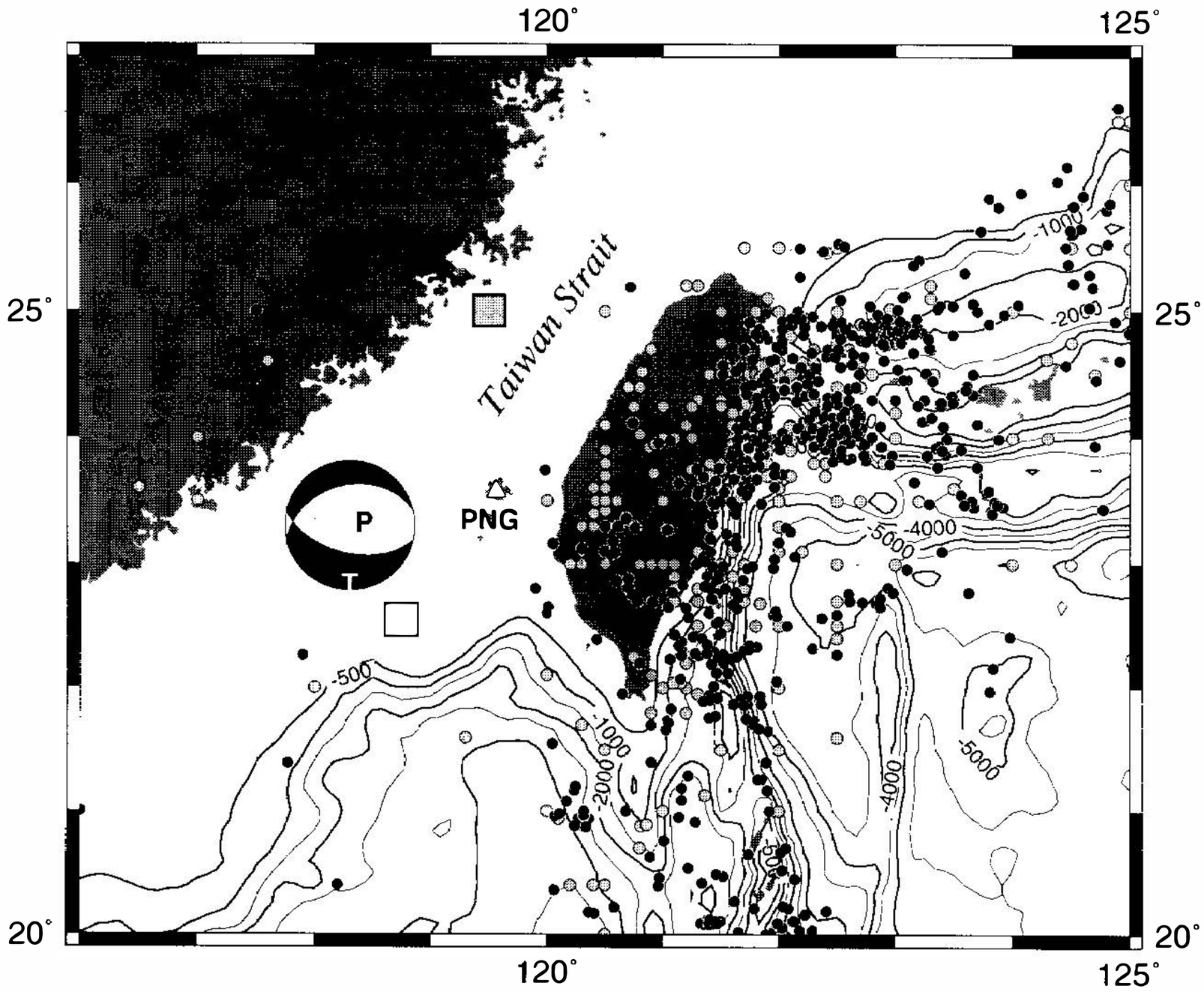

Fig. 2. Map showing historical seismicity (small gray dots), present seismicity (small black dots), and the epicenter of the 16 September 1994 earthquake (open square). Historical earthquakes were taken from the Global Hypocenter Data Base CD-ROM with an estimated magnitude equal to or greater than 6.0, while present earthquakes are those taken from bulletins of the International Seismological Center (ISC) and the Preliminary Determination of Epicenters (PDE) with $m_b \geq 4.9$. The largest event occurred in the region (the 1604 Quanzhou earthquake, M$\sim$8.0) is represented by a gray square. Equal-area projection of the lower hemisphere of the focal sphere is plotted showing the nodal planes, the P- and T-axes. Our result shows a high-angle, dip-slip normal faulting mechanism with nodal planes striking approximately eastwest. Bathymetric contours are meters below sea level.

in the north and the Tainan Basin in the south. These are separated by the Penghu Uplift, with the smaller Penghu Basin located to the west (Figure 1). The 16 September 1994 earthquake took place within the western part of the Tainan Basin, as marked by the open square in Figures 1 and 2. Based on seismic stratigraphy, Lee *et al.* (1993b) and Lee and Lawver (1994) concluded that the initiation of the Tainan Basin in Early Oligocene ($\sim$32 Ma) was directly related to the opening of the South China Sea. Widespread NE-SW-striking normal faulting accompanied the continental rifting in the region as a whole (Yu, 1990, 1993), and in the Taihsi Basin (Huang *et al.*, 1993) and in the Penghu Basin (Chang, 1992) in particular. By Middle Miocene ($\sim$13 Ma), the spreading of the South China Sea ceased, and the development of the Tainan Basin turned to the post-rift phase of thermal subsidence (Lee and Lawver, 1994; Lee *et al.*, 1993b; Yu, 1990, 1993). In the late Pliocene time ($\sim$5

Ma), when the North Luzon Arc began to collide with the South China continental margin (the Penglai Orogeny), the Tainan Basin began another stage of rapid subsidence (Lee *et al.*, 1993b). Unlike its previous phases, however, the latest subsidence is associated with the arc-continent collision (Lee *et al.*, 1993b; Yu, 1993).

According to the detailed petroleum exploration made by the Chinese Petroleum Corporation (CPC) in the seventies and eighties (Yang *et al.*, 1991; Yu, 1990), the Tainan Basin consists of two opposing and partly overlapping half-graben systems with the low relief accommodation zone (LRAZ) in between. These faults are considered to have been inactive since Late Pleistocene ($\sim$0.5 Ma) based on the termination of fault traces on seismic profiles (Yang *et al.*, 1991). Such a conclusion was consistent with the apparent lack of seismicity in terms of $m_b \geq 4.5$ events (Global Hypocenter Data Base CD-ROM, 1994), but the occurrence of the 16 September 1994 event proved it to be otherwise.

It is quite interesting to note that, while southern China is one of the least seismic areas of continental China, there have been major earthquakes in the portion of southeast coast of China near Taiwan. The largest earthquakes occurred in the region was the 1604 Quanzhou event with an estimated magnitude of 8.0 (Figure 2, Lee *et al.*, 1976, 1978). Historical events with magnitude greater than 6.0 distributed mainly near the coast of southeast China and on the island of Taiwan (Figure 2, Lee *et al.*, 1976, 1978). It is quite possible that the lack of historical large events in the Taiwan Strait, particularly in the Tainan and Taihsi basins, is an artifact due to the impossibility of pinpointing Strait earthquakes using historical documents, although this argument has no way to be verified.

3. WAVEFORM INVERSION FOR SOURCE PARAMETERS

In this section, we discuss in detail the source parameters of the 16 September 1994 event. Because of its large magnitude, good waveforms were recorded at nearly all stations around the globe. The recent addition of many broadband stations of the Global Seismic Network (GSN) provides excellent azimuthal coverage on the focal sphere, resulting in tight constraints on the focal parameters. This is in contrast to the poor resolution in source parameters based only on the CWB data, because the event is outside of the network (Figure 2). Therefore, we chose to determine the source parameters by inverting the body waveforms recorded at teleseismic distances. An added benefit of using teleseismic inversion is, of course, the capability of determining the centroid depth. Before we present our inversion result, we first briefly describe the teleseismic data and analysis procedures used.

3.1 Data and Analysis

All digital waveform data were transferred electronically from the Data Management Center of the Incorporated Research Institutions for Seismology (DMC, IRIS), which serves as the primary distributor of the GSN data. *P*- and *S*-waves recorded at epicentral distances of 30°-90° and 30°-70°, respectively, were used for our inversion to avoid the complexities from waves traveling through the upper mantle within 30° and possible interference with phases reflected off the core-mantle boundary (e.g., *PcP* and *ScS* waves) beyond 90° or 70°. Broadband *S* waveforms on the N-S and E-W components at each station were first rotated to radial and tangential directions to produce the tangential *SH* component. Then the *P* and *SH* ground displacements were obtained by deconvolving the broadband instrument response from respective seismograms. The seismic velocity model for the source region consists of a

mantle half space overlain by a 15-km crust and a thin (150 m) water layer. The *P*- and *S*-wave velocities for the mantle and crust are adopted from the IASPEI91 model (Kennett and Engdahl, 1991). Incidentally, changes in water depth, crustal velocities and Moho depth do not seem to affect our source inversion results very significantly. The attenuation constant, t*, is assumed to be 1 for *P* and 4 for *S* phases (Nábelek, 1984). Our formal inversion technique is based on the algorithm developed by Nábelek (1984) and later modified by Glennon and Chen (1993). The earthquake source is parameterized by a sequence of subevents where each subevent is represented by a centroidal solution (point source) constrained to be a pure double couple (Aki and Richards, 1980). Source parameters, including the focal mechanism (strike, dip, rake), focal depth, scalar seismic moment, relative amplitudes of the triangular segments composing the far-field source time function, and location and time delay of the centroid of the particular subevent relative to either the nucleation point or to the centroid of the first subevent, are inverted by simultaneously minimizing the difference between the observed and synthetic seismograms for both *P*- and *SH*-waves in a least squares sense. The seismograms were all normalized to an epicentral distance of 40° and a peak magnification of 1500. For each station, weight was assigned to compensate for bias introduced from uneven coverage of the focal sphere and to balance the amplitude differences between *P*- and *SH*-waves. Realistic uncertainties were estimated by systematically searching the parameter space around the best fitting solution through forward modeling. The allowable range for each parameter was determined by a noticeable increase in the root-mean-squared (rms) error of 5-10%.

3.2 Inversion Result

All the *P* phases used in our inversion show down-going first motions, suggesting that the 16 September 1994 event is associated with a normal fault. Indeed, our inversion result yields a normal faulting mechanism with both nodal planes trending approximately E-W (Table 1 and Figures 2 and 3). Such a mechanism is consistent with the N-S extension in the source region, as marked by the location of the maximum tension axis (i.e., the *T*-axis, Figures 1-3). Centroid-moment-tensor (CMT) solutions based on the inversion of long-period body ($\geq$45 s) and surface ($\geq$125 s) waves for this event were also available from several research groups through computer networks. Those solutions, including the ones reported by Harvard University (Dziewonski *et al.*, 1981), the Earthquake Research Institute (ERI) of the University of Tokyo (Kawakatsu *et al.*, 1994), and the USGS (Sipkin, 1982, 1986), are listed in Table 1 along with ours. While the mechanisms reported by the Harvard group and the ERI are similar to our best fitting solution, the strike determined by the USGS varies from ours by as much as 50°. Although the data provide better constraints on dip than on the strike and rake for this particular mechanism, a solution with nodal planes trending NW-SE is obviously beyond the acceptable range (Table 1).

A well-known weakness of CMT solutions using long period waves is the lack of resolution for very shallow earthquakes (Dziewonski *et al.* 1981; Sipkin, 1986). Thus, a fixed focal depth of 15 or 33 km is reported by the Harvard group whenever the actual depth is too shallow to be resolved. This turns out to be the case for the 16 September 1994 event (33 km). The reported depths by the ERI and the USGS are 23 and 22 km, respectively. All three values are significantly deeper than our final result of 13$\pm$3 km (Table 1). To assess the depth resolution of our analysis and the possible trade-off between the focal depth and the source time function (Christensen and Ruff, 1985), synthetic seismograms were generated

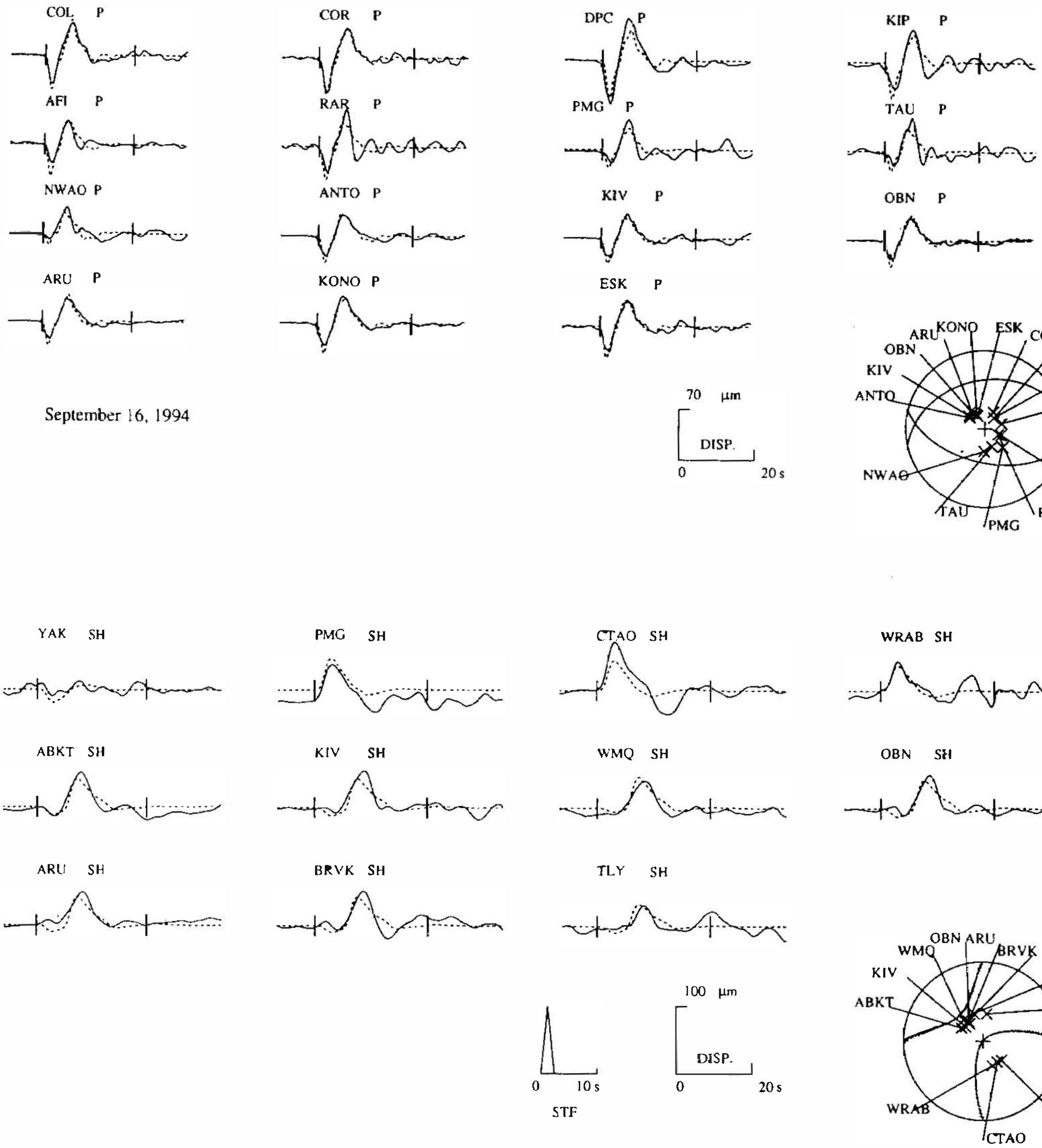

September 16, 1994

Fig. 3. Inversion result of the 16 September 1994 earthquake occurred in the Taiwan Strait. The observed (solid curves) and synthetic (dashed curves) ground displacements are plotted with the same scale. The seismic wave speeds (in km s^{-1}) and density (in g cm^{-3}) are 6.08 (P), 3.52 (S), and 2.67 for the crust, and 8.04, 4.47, and 3.35 for the mantle half-space, respectively. Orientations of the nodal surfaces for the direct P and SH phases and the locations of observations on the focal spheres are shown in equal-area projections of the lower hemisphere of the focal sphere. Vertical bars on the seismograms indicate time windows used in the inversion. The shape of the source time function (STF) is plotted near the bottom.

Table 1. Source Parameters* of the 16 September 1994 Earthquake.

Ref+	Origin Time (hr:min:sec)	Lat. °N	Long. °E	Depth km	Strike deg	Dip deg	Rake deg	Moment x 10^{18} Nt m
PDE	6:20:18.7	22.53	118.71	13	-	-	-	-
CWB	6:20:15.6	22.43	118.47	19.1	-	-	-	-
Harvard	-	-	-	33	100	50	-86	10.3
ERI	-	-	-	23	98	55	-85	11.4
USGS	-	-	-	22	155	67	-73	21
This study	-	-	-	13±3	103±17	55±5	-74±16	7.0±1.1

* Only the parameters of the preferred fault plane are listed; the parameters of the other plane can be derived from the given ones.

\+ PDE: Preliminary Determination of Epicenters; CWB: Seismological Center of the Central Weather Bureau of Taiwan; Harvard: Harvard University (Dziewonski *et al.*, 1981); ERI: Earthquake Research Institute of the University of Tokyo (Kawakatsu *et al.*, 1994); USGS: U. S. Geological Survey (Sipkin, 1982, 1986).

with a depth fixed at 23 km while all other parameters, including the duration and shape of the source time function, were allowed to vary. As shown in Figure 4, the larger depth is clearly inconsistent with the deconvolved broadband waveforms. It is noted that the depth reported by the PDE is the same as ours, while that by the CWB is ~6 km deeper at 19.1 km. Being outside of the network, the resolution of the CWB is probably not good either.

The source time function for this event is remarkably simple with a triangle of 2.4 s in duration (Figure 3). Clean P and SH waveforms along all azimuths suggest that most of the energy in these waves can be adequately explained by the direct arrival and surface-reflected phases (e.g., pP, sP, sS) and that more than one subevent is unwarranted. The scalar seismic moment is estimated to be $7.0 \pm 1.1 \times 10^{18}$ Nt m, which is somewhat smaller than those estimated by the CMT methods ($1\text{-}2 \times 10^{19}$ Nt m, Table 1); the discrepancy in moment release is probably due to the long-period energy release of the source more than 5 seconds after the origin time that is included in the long period surface waves, but not in the body wave phases used in our study.

3.3 Fault Orientation and Stress Drop

Figure 5 shows the distribution of the 3-day aftershocks of the 16 September 1994 event reported by the CWB of Taiwan. To identify which nodal plane was the actual fault plane, projection of hypocenters on cross sections was generated along various azimuths. The fact that the epicentral area is at least 140 km out of the local seismic network, however, inevitably causes a large degree of uncertainty in the determination of the hypocenters. Because of this, even the joint hypocenter determination (JHD, Douglas, 1967; Dewey 1972) may not provide significant improvement. Nonetheless, the distribution of hypocenters seems to suggest a high-angle, south-dipping fault plane striking ~N100°E (see cross-section B-B′ in Figure 5). When comparing to our fault plane solution, it is inferred that the normal faulting earthquake took place on the plane with strike and dip of 103° and 55°, respectively.

Determination of the stress drop associated with an earthquake requires a priori knowledge of the fault geometry in addition to the seismic moment and source time function determined from waveform inversion. By assuming a circular dislocation model, Brune (1970, 1971) calculated the stress drop, $\Delta\sigma$, to be:

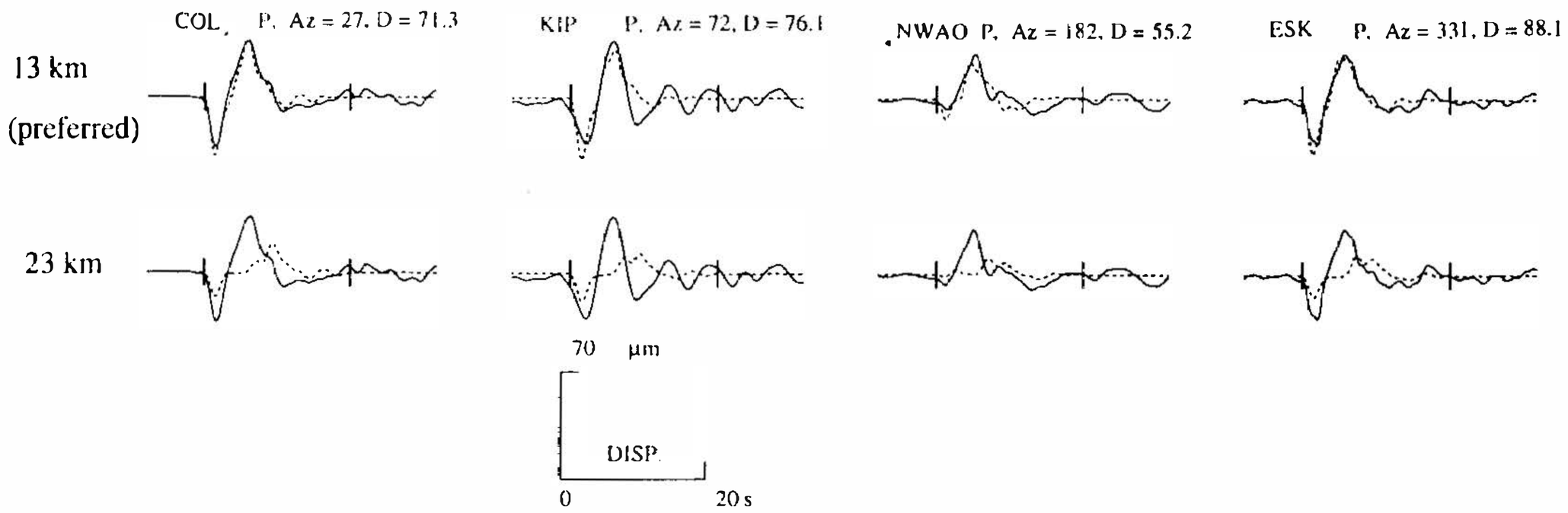

Fig. 4. Comparison of selected waveforms along various azimuths generated with a focal depth of 13 km (our best fitting solution, top) and 23 km (CMT solutions, bottom). The deeper depth is clearly rejected by waveform data.

$$\Delta\sigma = \frac{7\pi}{16}\frac{\mu D}{r} = \frac{7\pi}{16}\frac{\mu DA}{rA} = \frac{7}{16}\frac{M_o}{r^3} \tag{1}$$

where μ is the rigidity of source material, D is the average dislocation, r is the radius of the fault in km, A is the fault area (i.e., πr^2), and M_o is the seismic moment (i.e., $\mu\ D\ A$, by definition). For a rectangular fault geometry, we can calculate the "equivalent" radius by assuming the same rupture area (Chung and Kanamori, 1980), i.e.,

$$r = \pi^{-1/2}(LW)^{1/2} \tag{2}$$

where L and W are the rupture length and width, respectively.

In the case when only the far-field source time function rather than the fault geometry is known, Fukao and Kikuchi (1987) assumed the rupture area to be the square of the product of the half duration of the source time function ($\tau_{1/2}$) and the rupture velocity (ν),

$$\pi r^2 = (\nu\tau_{1/2})^2, \quad r = \pi^{1/2}\nu\tau_{1/2} \tag{3}$$

Substituting (3) into (1) yields

$$\Delta\sigma \approx 2.5\frac{M_o}{(\nu\tau_{1/2})^3} \tag{4}$$

This is essentially the formula used by Kickuchi and Fukao (1988) and Sugi *et al.* (1989).

For the 16 September 1994 event in the Taiwan Strait, the distribution of aftershocks does not give a clear indication of the fault dimension (Figure 5). If we assume that the area with the highest density of aftershocks is the fault zone, then L and W are estimated to be 15 and 20 km, respectively. Using (1) and (2), we calculated the corresponding stress drop to be 33 bar.

On the other hand, if we use (3) and (4) with $\tau_{1/2}$ and ν being 1.2 s and 3 km s^{-1}, respectively, then the calculated stress drop is nearly 3.8 kbar. Considering that the lithospheric pressure at the source depth ($\sim$13 km) is only about 3.9 kbar, such a high value

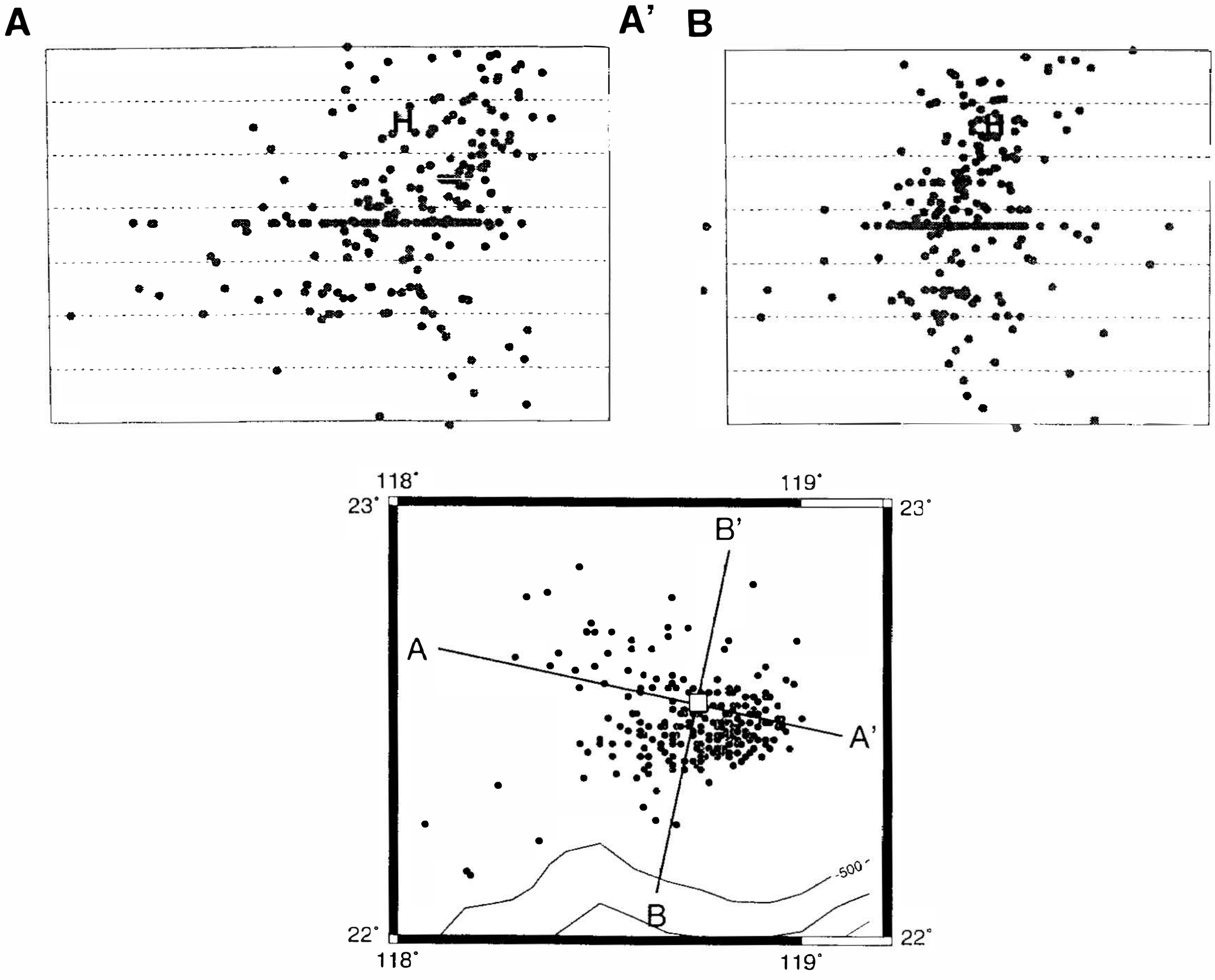

Fig. 5. Three-day aftershock distribution (small dots) of the 16 September 1994 earthquake (open square). Epicenters were reported by the Seismological Center of the Central Weather Bureau (CWB). Uncertainty in the hypocentral locations is expected to be large due to the incomplete focal coverage by the local network. Cross-sections are made along various azimuths with an "H" marking the projected location of the main shock. Particularly along the profile B-B′, the distribution of aftershocks seems to suggest a south-dipping fault plane.

means that the source region is virtually free from any stress after the earthquake, a very unlikely case. Even when we allow the maximum trade-off between the focal depth and the source time function such that the source duration is 50% longer, the calculated stress drop is ~1.1 kbar, still much higher than the 33 bar estimated from the rupture area. Obviously, independent verification seems necessary to distinguish these paradoxical estimations of stress drop. According to the w-2 model (Brune, 1970, 1971; Kikuchi and Fukao, 1988), the corner frequency (f_c) of the far-field source spectrum after correcting for the attenuation and geometrical spreading is proportional to the cubic root of stress drop. That is,

$$f_c \approx 0.49\beta\left(\frac{\Delta\sigma}{M_o}\right)^{1/3} \tag{5}$$

where β is the shear wave speed of the source material (3.52 km s^{-1} in our case). Therefore, a stress drop of 33 bar should correspond to a corner frequency of 0.13 Hz while 3.8 kbar to 0.65 Hz. Figure 6 is the *SH* component of the broadband strong-motion data recorded on the island of Penghu (PNG, Figure 1) approximately 140 km northeast of the epicenter, the closest broadband seismogram available for this event. The displacement spectrum is for a 30-second window after the first arrival to ensure the inclusion of *S*-related phases (Kanamori *et al.*, 1993). Although the spectrum seems to suggest a corner frequency of around 0.65 Hz, a lower value cannot be completely ruled out.

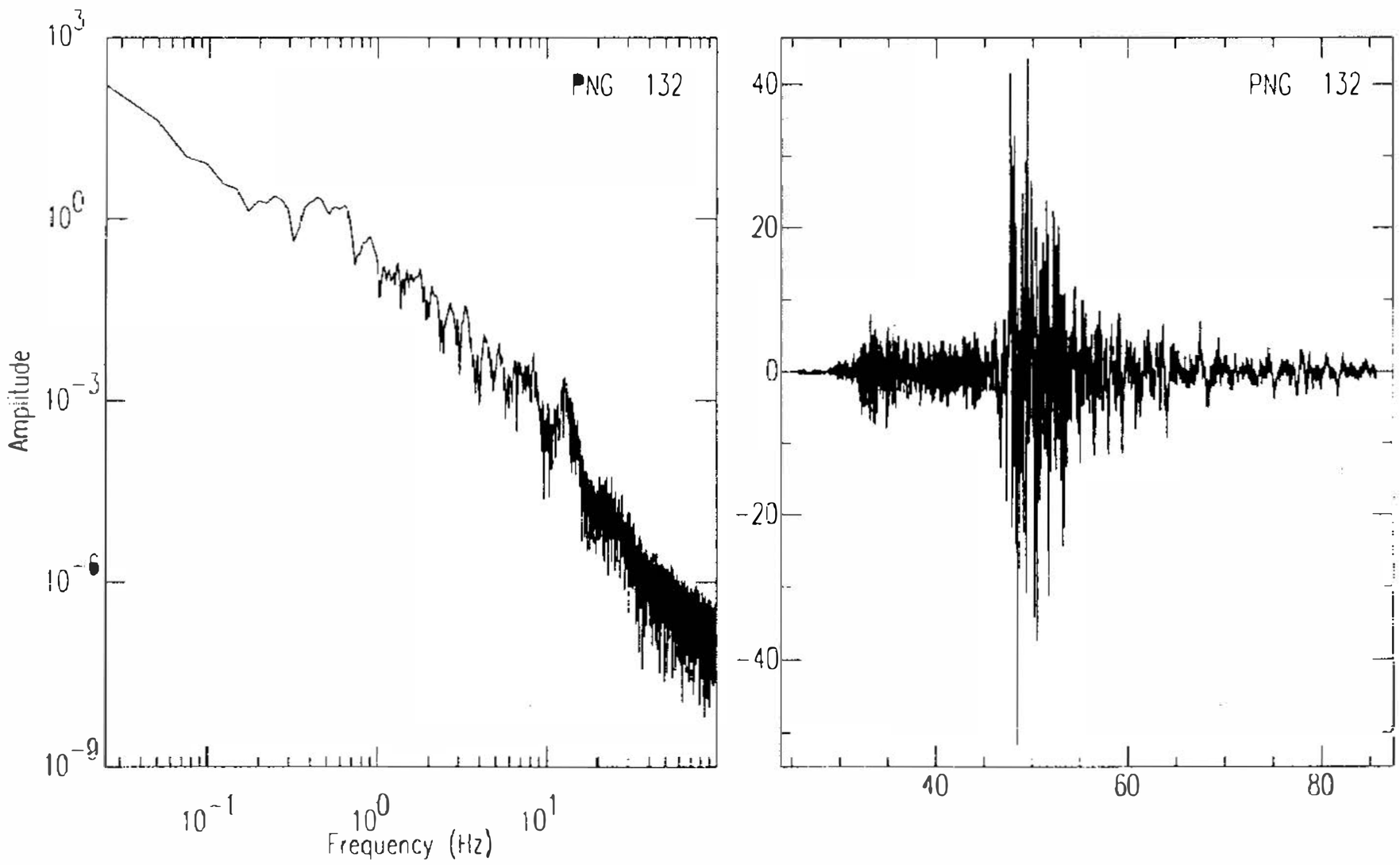

Fig. 6. Broadband strong-motion seismogram recorded at PNG approximately 140 km northeast of the epicenter. The original acceleragrams were rotated to the great circle path to delineate the SH component (right). The displacement spectrum corresponding to a 30-s window after the first arrival is shown on the left. Notice that a corner frequency of 0.65 Hz, predicted by the calculated stress drop is consistent with the observation although lower values cannot be completely ruled out.

4. TECTONIC IMPLICATION AND DISCUSSION

The occurrence of the 16 September 1994 earthquake clearly demonstrates that the EW striking faults in the Taiwan Strait, including those mapped by multichannel profiling, are potentially all active. We do not have data to accurately associate a fault with this earthquake, but the proximity of the mapped structures to the epicenter raises the possibility that the mapped faults may go down to a depth of more than 10 km at a fairly high angle

rather than becoming listric, as is often assumed. Not only is the implication of such active faults on the petroleum resources important, it also has direct implication on the collision tectonics of Taiwan.

The problem of producing normal faulting in an otherwise compressional environment has attracted the attention of tectonophysicists and field geologists (England and Molnar, 1993; Burchfiel and Royden, 1985). Normal faulting occurs in two different environments. One of them is on high plateaus on one side of a collision zone, such as in Tibet (Molnar and Tapponier, 1978; Armijo, 1986), or Andes (Mercier *et al.*, 1992); in such cases, the strike of the fault is nearly parallel to the maximum compressional axis due to collision, σ_1. The other type has been found in high ranges where, as is the case with the Himalayas and Andes, underthrusting occurs at depth; in this case the strike is parallel to that of the compressional mountain belt. The latter type has been found abundantly in the high Himalayas (Burchfiel *et al.*, 1992) as well as in the Central Range of Taiwan (Crespi, 1995). As judged by the epicentral location, the 16 September 1994 earthquake occurred in a different environment from the ones just discussed. Here, normal faulting takes place at a distance away from the collisional boundary that it is *not* associated with a plateau or a high range with underthrusting underneath.

The occurrence of normal faulting does require that the vertical stress becomes the maximum stress in some way. England and Molnar (1993) suggested that in Tibet it is the delamination in the upper mantle that led to rapid rising and normal faulting; as alternatives they also suggested that normal faulting may ensue the cessation of compression and/or uplifting. For the Taiwan Strait, none of these mechanisms can explain the normal faulting there. For if this tectonic phenomenon is related to the collision, since no other active tectonic forces can be invoked, the cessation of collision is not possible in view of rapid convergence as determined by the GPS campaign and the frequent occurrence of earthquakes near Taiwan. The lack of any significant topography in the epicentral area does not allow us to resort to elevation-driven increase in gravitational energy either. Other mechanisms must be sought.

To activate the normal faulting, assuming that the collision is eventually responsible for it, the magnitude of the collision-related stress, σ_1, has to decrease in magnitude until it is less than the over-burden pressure. It is possible that the collisional stress has been significantly absorbed by the deformation associated with the orogeny and, therefore, attenuated to a relatively low value in the vicinity of the 16 September 1994 epicenter, as the distance to the collision boundary is more than 200 km. However, we still need to make sure that σ_3 turns N-S there. Since it is difficult to invoke any process in the crust to do so, and we do have to account for the excess mass in the mantle as the Philippine Sea plate continues to press westward and Taiwan is shortened in the process, it is conceivable that the viscous mantle has to flow in a nearly NS direction, if there is a resistance further to the west from the more stable continental interior of SE Chinese mainland. We may offer the hypothesis that it is this NS flow in the upper mantle that led to normal faulting in the Taiwan Strait. To test this hypothesis further, we evidently need to model this flow and investigate the state of stress in the crust above by measuring seismic velocity anisotropy in the Strait area either using SKS (Silver and Chan, 1991) or surface waves (Yu *et al.*, 1994). If this mechanism we propose to explain the normal faulting observed in Taiwan Strait is correct, it may also be worthwhile to reexamine the mechanism that led to the N-S striking normal faults on high plateaus: Are they necessarily related to the elevation of the plateau?

The occurrence of this earthquake has thrown an open question on the role of the Taiwan Strait in the overall Taiwan collisional tectonics. In the thin-skinned hypothesis many of the

actions take place in the critically tapered wedge (Barr and Dahlen, 1990; Dahlen *et al.*, 1984; Suppe, 1981), while the underlying lower crust and the upper mantle under western Taiwan is viewed as a subducting continental lithosphere. In such a model, the Strait should correspond to the outer-rise. Consequently, the normal faulting should have its maximum tension axis (i.e., T-axis) perpendicular to the trend of the island, clearly not consistent with our observation. In fact, the E-W trending normal faults in the Tainan Basin are mapped continuously from southwestern Taiwan to the middle of the Strait (e.g., Huang *et al.*, 1993; Lee *et al.*, 1993a, 1993b; Yang *et al.*, 1991; Yu, 1990), and this system of faults is not easily explainable in terms of a shallow wedge deformation. It seems that a model including dynamics in the crust and the upper mantle is necessitated.

The stress-drop values obtained demonstrate the sensitivity of such calculations to the assumed fault dimensions. A high stress-drop is not inconsistent with the fact that the area has not been subjected to repeated large earthquakes in recent years and, therefore, high-stress events are likely. This question cannot be addressed adequately at present because the event is too far outside of the CWB network such that mapping the source zone in detail is impossible.

5. CONCLUSIONS

The 16 September 1994 earthquake is the largest event (m_b=6.5) which has occurred in the Taiwan Strait since modern seismic observations became available for the region. The epicenter is located about 150 km southwest of Taiwan in the Tainan Basin. In the Taiwan Strait, the continental rifting that occurred between ~32 and 13 Ma that created many NE-SW striking normal faults and the thermal subsidence in later time have long ceased to be active. The Tainan Basin, as mapped by petroleum exploration, seems to be excluded from both historical and recent significant seismicity. This earthquake has made it clear that the Strait as a whole is seismically active and that events of this magnitude or higher (e.g. matching that of the 1604 Quanzhou earthquake) may indeed occur in the future.

We determined the source parameters of the 16 September 1994 earthquake by inverting both *P* and *SH* body waveforms recorded at teleseismic distances. Ground displacements were obtained by deconvolving the instrument response from broadband seismograms. Our best fitting solution shows a normal faulting mechanism with high-angle nodal planes striking approximately east-west (strike, 103±17; dip, 55±5; rake, -74±16). The direction of the maximum tension axis is north-south, approximately parallel to the structural trend on the island of Taiwan. The centroidal source depth is estimated to be 13±3 km which is consistent with that reported by the Preliminary Determination of Epicenter (PDE). The significantly deeper depths reported by several groups using the centroid-moment-tensor (CMT) technique are evidently overestimated due to insufficient resolution. The source time function is a simple triangle of only 2.4 s in duration, whereas the seismic moment is $7.0\pm1.1 \times 10^{18}$ Nt m.

Because nearly all local stations are located in the same quadrant, relatively large uncertainty in hypocentral locations of aftershocks is inevitable. A south-dipping nodal plane is considered to be the actual fault plane based on aftershock distribution, although further verification is needed. By assuming the rupture area to be the zone with the densest distribution of aftershocks, its width and length are estimated to be ~20 and ~15 km, respectively. Such a geometry would result in a calculated stress drop of ~33 bar. However, the calculated stress drop is as high as 3.8 kbar if the rupture area is assumed to be the

square of the product of the half duration of the source time function and the rupture velocity (Kikuchi and Fukao, 1988). The corner frequency of the displacement spectrum recovered from the broadband seismogram recorded at the closest station (PNG) is consistent with the higher value, but lower stress drops cannot be ruled out either.

The normal faulting evidently is a result of north-south extension, nearly perpendicular to the relative motion between the Philippine Sea plate and the Eurasia plate. The geometry is quite analogous to the formation of the graben in the high Tibet plateau behind the Himalaya collision zone with the motion vector of the Indian plate nearly perpendicular to the extension. The arc-continent collision near Taiwan is not as grand either in scale or in intensity, when compared to the continent-continent collision in the Himalayas, but the occurrence of the 16 September 1994 event suggests that similar patterns of stress/strain fields are observed behind the collision zones for both regions. None of the previously suggested mechanisms of graben-formation on high plateaus can be invoked to explain the occurrence of this earthquake since the event occurred under shallow sea. Nor can this event be explained as an outer-rise bending earthquake associated with the eastward subduction along the Manila trench, either. We propose that northsouth mantle flow under the crust in the Taiwan Strait may be able to create a condition favorable for nearly eastwest striking normal faults to occur.

Acknowledgments The authors thank J. Nábelek for a copy of his inversion routines. The regular posts of CMT solutions by the Harvard group, POSEIDON data center, and the USGS on Internet are gratefully acknowledged. We also benefited from discussions with W.-P. Chen, B.-Y. Kuo, B.-S. Hwang, and W.-T. Liang. This research is supported by grant NSC83-0202-M-001-010 from the National Science Council of Taiwan, Republic of China.

REFERENCES

Aki, K., and P. G. Richards, 1980: Quntitative seismology: Theory and methods. Freeman, San Francisco, 932pp.

Armijo, R, P. Tapponnier, J. L. Mercier, and T. Han, 1986: Quaternary extension in southern Tibet: Field observations and tectonic implications. *J. Geophys. Res.*, **91**, 13,803-13,872.

Barr, T. D., and F. A. Dahlen, 1990: Constraints on friction and stress in the Taiwan fold-and-thrust belt from heat flow and geochronology. *Geology*, **18**, 111-115.

Bowin, C., R. S. Lu, C. S. Lee, and H. Schouton, 1978: Plate convergence and accretion in the Taiwan-Luzon region. *AAPG Bull.*, **62**, 1645-1672.

Brune, J. N., 1970: Tectonic stress and the spectra of seismic shear waves from earthquakes. *J. Geophys. Res.*, **75**, 4997-5009.

Brune, J. N., 1971: Correction. *J. Geophys. Res.*, **76**, 5002.

Burchfiel, B. C., and L. H. Royden, 1985: North-South extension within the convergent Himalayan region. *Geology*, **13**, 679-682.

Burchfiel, B. C., Z. L. Chen, K. V. Hodges, Y. P. Liu, and L. H. Royden, 1992: The south Tibetan detachment system, Himalayan orogen: Extension contemporaneous with and parallel to shortening in a collisional mountain belt. *Geol. Soc. Am. Special Papers*, p.269.

Chang, M., 1992: Integrated geological and geophysical interpretation of the Penghu sedimentary basin. *Petrol. Geol. Taiwan*, **27**, 237-250.

Christensen, D. H., and L. J. Ruff, 1985: Analysis of the trade-off between hypocentral depth and source time function. *Bull. Seism. Soc. Am.*, **75**, 1637-1656.

Chung, W.-Y., and H. Kanamori, 1980: Variation of seismic source parameters and stress drops within a descending slab and its implications in plate mechanics. *Phys. Earth Planet. Inter.*, **23**, 134-159.

Crespi, J., 1995: Deformation partitioning at shallow crustal levels in the Taiwan arc-continent collision. Int'l Conference and 3rd Sino-French Symposium on Active Collision in Taiwan: Program and Extended Abstracts, 71-76.

Dahlen, F. A., J. Suppe, and D. M. Davis, 1984: Mechanics of fold-and-thrust belts and accretionary wedges: cohesive Coulomb theory. *J. Geophys. Res.*, **89**, 10,087-10,101.

Dewey, J. W., 1972: Seismicity and tectonics of western Venezuela. *Bull. Seism. Soc. Am.*, **62**, 1711-1751.

Dziewonski, A. M., T.-A. Chou, and J. H. Woodhouse, 1981: Determination of earthquake source parameters from waveform data for studies of global and regional seismicity. *J. Geophys. Res.*, **86**, 2825-2852.

England, P., and P. Molnar, 1993: Cause and effect among thrust and normal faulting, anatectic melting and exhumation in the Himalayas. *Geol. Soc. Am. Special Publication*, **74**, 401-411.

Fukao, Y., and M. Kikuchi, 1987: Source retrieval for mantle earthquakes by iterative deconvolution of long-period P-waves. *Tectonophysics*, **144**, 249-269.

Glennon, M. A., and W.-P. Chen, 1993: Systematics of deep-focus earthquakes along the Kuril-Kamchatka arc and their implications on mantle dynamics. *J. Geophys. Res.*, **98**, 735-769.

Global Hypocenter Data Base CD-ROM, 1994: National Earthquake Information Center, U. S. Geol. Surv.

Ho, C. S., 1986: A synthesis of the geologic evolution of Taiwan. *Tectonophysics*, **144**, 159-180.

Houseman, G., and P. England, 1993: Crustal thickening versus lateral expulsion in the Indian-Asian continental collision. *J. Geophys. Res.*, **98**, 12,233-12,249.

Huang, S.-T., R.-C. Chen, and W.-R. Chi, 1993: Inversion tectonics and evolution of the northern Taihsi basin, Taiwan. *Petrol. Geol. Taiwan*, **28**, 15-46.

Huchon, P., 1986: Comment on "Kinematics of the Philippine Sea plate: by B. Ranken, R. K. Cardwell, and D. E. Karig. *Tectonics*, **5**, 165-168.

Kanamori, H., J. Mori, E. Hauksson, T. Heaton, L. K. Hutton, and L. M. Jones, 1993: Determination of earthquake energy release and M_L using TERRAscope. *Bull. Seism. Soc. Am.*, **83**, 330-346.

Karig, D. E., and R. K. Cardwell, 1986: Reply to "Comment on 'Kinematics of the Philippine Sea plate' by B. Ranken, R. K. Cardwell, and D. E. Karig". *Tectonics*, **5**, 169-170.

Kawakatsu, H., K. Takano, S. Tsuboi, and Y. Yamanaka, 1994: Automated pseudo-realtime CMT inversion (abstract). *EOS Trans. AGU*, **75**, p.234.

Kennett, B. L. N., and E. R. Engdahl, 1991: Traveltimes for global earthquake location and phase identification. *Geophys. J. Int.*, **105**, 429-465.

Kikuchi, M., and Y. Fukao, 1988: Seismic wave energy inferred from long-period body wave inversion. *Bull. Seism. Soc. Am.*, **78**, 1707-1724.

Lee, T.-Y., and L. A. Lawver, 1994: Cenozoic plate reconstruction of the South China Sea region. *Tectonophysics*, **235**, 149-180.

Lee, W. H. K., F. T. Wu, and C. Jacobsen, 1976: A catalog of historical earthquakes in China. *Bull. Seism. Soc. Am.*, **66**, 2003-2016.

Lee, W. H. K., F. T. Wu, and S. C. Wang, 1978: A catalog of instrumentally determined earthquakes in China (magnitude 6 and larger) compiled from various papers. *Bull. Seism. Soc. Am.*, **68**, 383-398.

Lee, C.-I., Y.-L. Chang, E.-W. Mao, and C.-S. Tseng, 1993a: Fault reactivation and structural inversion in the Hsinchu-Miaoli area of northern Taiwan. *Petrol. Geol. Taiwan*, **28**, 47-58.

Lee, T.-Y., C.-H. Tang, J.-S. Ting, and Y.-Y. Hsu, 1993b: Sequence stratigraphy of the Tainan basin, offshore southwestern Taiwan. *Petrol. Geol. Taiwan*, **28**, 119-158.

Minster, J. B., and T. H. Jordan, 1979: Rotation vectors for the Philippine and Rivera plates (abstract), *EOS Trans. AGU*, **60**, p.958.

Molnar, P., and P. Tapponnier, 1978: Active tectonics of Tibet. *J. Geophys. Res.*, **83**, 5361-5375.

Nábelek, J. L., 1984: Determination of earthquake source parameters from inversion of body waves. Ph.D. Thesis, Mass. Inst. of Technol., Cambridge. 309pp.

Ranken, B., R. K. Cardwell, and D. E. Karig, 1984: Kinematics of the Philippine Sea plate. *Tectonics*, **3**, 555-575.

Rau, R.-J., and F. T. Wu, 1995: Tomographic imaging of lithospheric structures under Taiwan. *Earth Planet. Sci. Lett.*, **133**, 517-532.

Roecker, S. W., Y. H. Yeh, and Y. B. Tsai, 1987: Three-dimensional P and S wave velocity structures beneath Taiwan: deep structure beneath an arc-continent collision. *J. Geophys. Res.*, **92**, 10,547-10,570.

Seno, T., 1977: The instantaneous rotation vector of the Philippine Sea plate relative to the Eurasian plate. *Tectonophysics*, **42**, 209-229.

Seno, T., T. Moriyama, S. Stein, and D. F. Woods, 1987: Redetermination of the Philippine Sea Plate motion (abstract). *EOS Trans. AGU*, **68**, p.1474.

Seno, T., S. Stein, and A. E. Gripp, 1993: A model for the motion of the Philippine Sea Plate consistent with NUVEL-1 and geological data. *J. Geophys. Res.*, **98**, 17,941-17,948.

Silver, P. G., and W. W. Chan, 1991: Shear wave splitting and subcontinental mantle deformation. *J. Geophys. Res.*, **96**, 16,429-16,454.

Sipkin, S. A., 1982: Estimation of earthquake source parameters by the inversion of waveform data: synthetic waveforms. *Phys. Earth Planet. Inter.*, **30**, 242-259.

Sipkin, S. A., 1986: Estimation of earthquake source parameters by the inversion of waveform data: global seismicity, 1981-1983. *Bull. Seism. Soc. Am.*, **76**, 1515-1541.

Sugi, N., M. Kikuchi, and Y. Fukao, 1989: Mode of stress release within a subducting slab of lithosphere: implication of source mechanism of deep and intermediate-depth earthquakes. *Phys. Earth Planet. Inter.*, **55**, 106-125.

Suppe, J., 1981: Mechanics of mountain building and metamorphism in Taiwan. *Geol. Soc. China Mem.*, **4**, 67-89.

Teng, L. S., 1990: Geotectonic evolution of late Cenozoic arc-continent collision. *Tectonophysics*, **183**, 57-76.

Wu, F. T., 1978: Recent tectonics of Taiwan. *J. Phys. Earth*, **26**, S265-299.

Wu, F. T., D. Salzberg, and R. J. Rau, 1991: The modern orogeny of Taiwan, TAICRUST Workshop Proc., National Taiwan Univ., Taipei, 49-62.

Yang, K.-M., H.-H. Ting, and J. Yuan, 1991: Structural styles and tectonic modes of Neogene extensional tectonics in southwestern Taiwan: Implications for hydrocarbon exploration. *Petrol. Geol. Taiwan*, **26**, 1-31.

Yu, H.-S., 1990: Stratigraphy, structure and tectonic history of Tainan basin off southwest Taiwan. *Acta Ocean. Taiwan.*, **25**, 19-30.

Yu, H.-S., 1993: Contrasting tectonic style of a foredeep with a passive margin: southwest Taiwan and south China. *Petrol. Geol. Taiwan*, **28**, 97-118.

Yu, Y., J. Park, and F. T. Wu, 1995: Mantle anisotropy beneath the Tibetan plateau: evidence from long-period surface waves. *Phys. Earth Planet. Inter.*, **87**, 231-246.